Decorin Reduces Intraocular Pressure and Retinal Ganglion Cell Loss in Rodents Through Fibrolysis of the Scarred Trabecular Meshwork

Lisa J. Hill,[1] Ben Mead,[1] Richard J. Blanch,[1,2] Zubair Ahmed,[1] Felicity De Cogan,[1] Peter J. Morgan-Warren,[1] Shabbir Mohamed,[1] Wendy Leadbeater,[1] Robert A. H. Scott,[1,2] Martin Berry,[1] and Ann Logan[1]

[1]Neurotrauma Research Group, Neurobiology Section, Clinical and Experimental Medicine, University of Birmingham, Birmingham, United Kingdom
[2]Academic Department of Military Surgery and Trauma, Royal Centre for Defence Medicine, Birmingham, United Kingdom

Correspondence: Lisa J. Hill, Neurotrauma Research Group, Neurobiology Section, Clinical and Experimental Medicine, University of Birmingham, Birmingham, B15 2TT, UK; l.j.hill@bham.ac.uk.

Submitted: September 5, 2014
Accepted: May 1, 2015

Citation: Hill LJ, Mead B, Blanch RJ, et al. Decorin reduces intraocular pressure and retinal ganglion cell loss in rodents through fibrolysis of the scarred trabecular meshwork. *Invest Ophthalmol Vis Sci*. 2015;56:3743–3757. DOI:10.1167/iovs.14-15622

Purpose. To investigate whether Decorin, a matrikine that regulates extracellular matrix (ECM) deposition, can reverse established trabecular meshwork (TM) fibrosis, lower IOP, and reduce progressive retinal ganglion cell (RGC) death in a novel rodent model of TM fibrosis.

Methods. Adult rats had intracameral (IC) injections of human recombinant (hr) TGF-β over 30 days (30d; to induce TM fibrosis, raise IOP, and initiate RGC death by 17d) or PBS (controls) and visually evoked potentials (VEP) were measured at 30d to evaluate resultant visual pathway dysfunction. In some animals TGF-β injections were stopped at 17d when TM fibrosis and IOP were consistently raised and either hrDecorin or PBS IC injections were administered between 21d and 30d. Intraocular pressure was measured biweekly and eyes were processed for immunohistochemical analysis of ECM deposition to assess TM fibrosis and levels of matrix metalloproteinases (MMP) and tissue inhibitors of matrix metalloproteinases (TIMP) to assess fibrolysis. The effect of hrDecorin treatment on RGC survival was also assessed.

Results. Transforming growth factor–β injections caused sustained increases in ECM deposition in the TM and raised IOP by 17d, responses that were associated with 42% RGC loss and a significant decrease in VEP amplitude measured at 30d. Decorin treatment from 17d reduced TGF-β–induced TM fibrosis, increased levels of MMP2 and MMP9 and lowered TIMP2 levels, and lowered IOP, preventing progressive RGC loss.

Conclusions. Human recombinant Decorin reversed established TM fibrosis and lowered IOP, thereby rescuing RGC from progressive death. These data provide evidence for the candidacy of hrDecorin as a treatment for open-angle glaucoma.

Keywords: TGF-β, Decorin, extracellular matrix, intraocular pressure, trabecular meshwork, fibrolysis

Glaucoma describes a group of progressive optic neuropathies that have the potential to cause irreversible blindness in which a main risk factor is raised IOP. In POAG, increases in IOP occur when aqueous humour (AqH) outflow through the trabecular meshwork (TM) is reduced, usually as a result of abnormalities in TM cellularity,[1–4] TM contraction,[5,6] and extracellular matrix (ECM) levels.[4,7–9] The elastic-type fibers in the TM are surrounded by a sheath of fine fibrils embedded in an amorphous ECM made up of collagen IV, laminin, and fibronectin. The presence of plaque material associated with sheaths of the elastic-like fibers in the juxtacanalicular tissue (JCT) within the TM (Sheath-derived [SD] plaques) are also a pathological feature of POAG, with patients presenting with significantly more, and thicker, SD-plaques in their TM compared with eyes from age-matched controls.[4,10–12] These SD-plaques, however, are not thought to contribute to increased outflow resistance since Lujten-Drecoll et al.,[10] showed that eyes with psuedoexfoliation glaucoma had similar levels of SD-plaque material when compared with healthy eyes, but still had higher levels of IOP. Nevertheless, increased levels of ECM are seen around TM sheaths and this deposition could contribute to increased outflow resistance.[13] These cellular and ECM changes in the TM, together with altered TM cell contractile abilities result in a dysfunctional TM and ultimately loss of the tight control of AqH outflow.

The mechanisms that lead to TM dysfunction in POAG are probably multifactorial, but pathologically high levels of TGF-β within the AqH are thought to contribute.[9,14–24] Some POAG patients have elevated levels of TGF-β in their AqH compared with AqH taken from age-matched patients with cataracts[25–27] or other forms of glaucoma.[28] A role for TGF-β in increasing TM ECM deposition and IOP has been demonstrated by human eye perfusion experiments[29,30] and in rodent models of glaucoma.[16,20–22] Gene expression studies from cultured human TM cells also support the assertion that both TGF-β1 and TGF-β2 isoforms induce the overexpression of ECM proteins that may contribute to TM changes seen in glaucoma.[9,31,32] Additionally, TGF-β prevents the breakdown of ECM by inhibiting the activation of matrix metalloproteinases (MMP) through increasing levels of plasminogen

activator inhibitor (PAI)-1 and tissue inhibitors of metalloproteinases (TIMP). Plasminogen activator inhibitor–1 inhibits the conversion of plasminogen to plasmin, which is required for the plasmin-dependent activation of MMP.[14,18,33,34] The IOP-increasing effects of TGF-β have also been attributed to the cytokine's ability to reduce proliferation[35] and induce apoptosis of TM cells,[36] thereby reducing the overall numbers of TM cells.[19,24]

Transforming growth factor–β also stimulates contraction of TM cells through the RhoA-Rho kinase signaling pathway,[31] with TM contractility significantly influencing IOP.[37–39] Studies that have reduced or ablated RhoA-mediated TM contraction using Rho/ROCK inhibitors, have led to new classes of IOP lowering agents being considered to treat glaucoma.[37,40–42] However, it is unlikely that Rho/ROCK inhibitors alone can address the chronic fibrotic pathology that occurs in some patients with POAG, with their efficacy is still under scrutiny. Ultimately, IOP elevations lead to metabolic and biochemical changes in cells of the optic nerve head and retina,[43] which, together with the mechanical axonal compression that affects both retrograde and anterograde axonal transport depriving RGC of neurotrophic factors,[44] culminates in RGC apoptosis and optic disc cupping,[45,46] features that are diagnostic of glaucoma.

The multifactorial etiology of POAG makes accurate experimental modelling of the condition challenging. A major impediment to testing antifibrotic/fibrolytic agents that address TM fibrosis is the lack of reliable animal models that mimic the fibrotic etiology of POAG. Although not replicating the human condition perfectly, some current rodent models are useful for evaluating therapeutics that reduce IOP and prevent RGC death. For example, Junglas et al.[16] used adenovirus to overexpress the profibrotic connective tissue growth factor (CTGF, a downstream mediator of TGF-β effects) in order to demonstrate a link between CTGF and TM fibrosis associated with increased IOP and RGC loss, but they did not evaluate the efficacy of antifibrotic agents. Ideally, fibrolytic treatments would be better assessed in a chronic model of established TM fibrosis, whereby TM fibrosis is sustained without the need for continued administration of the profibrogenic agent.

The matrikine Decorin is a small leucine-rich proteoglycan that regulates cell proliferation, survival and differentiation by antagonizing growth factors and/or their receptors, including TGF-β,[47–49] epidermal growth factor (EGF),[50] vascular endothelial growth factor (VEGF),[51] insulin-like growth factor-I (IGF-I),[52] as well as directly interfering with collagen fibrillogenesis.[53] Decorin also increases MMP activity by increasing levels of tissue plasminogen activator (tPA), enabling cleavage of plasminogen to plasmin,[54,55] a step that is required for plasmin-dependent activation of MMP. Decorin also reduces PAI-1 and TIMP levels, further facilitating MMP activation.[54] Decorin's fibrolytic actions have been noted in many fibroproliferative pathologies, including proliferative vitreoretinopathy,[56] renal fibrosis,[57] lung fibrosis,[58] juvenile communicating hydrocephalus,[47] and spinal cord injury.[54,55,59]

Here, we investigated the fibrolytic properties of human recombinant (hr) Decorin in the fibrosed TM using a rodent model in which TM fibrosis is established by repeated intracameral injections (IC) of TGF-β, with the fibrosis being sustained upon withdrawal of the fibrogenic cytokine. We predicted that (1) TGF-β–induced fibrosis of the TM would permanently block AqH drainage, leading to increased IOP and death of RGC with measurable effects on retinal function, and (2) that treatment with hrDecorin would reduce established TM fibrosis, lower IOP and indirectly protect RGC against progressive death.

Methods

Animals and Surgery

Eight- to 10-week-old, male, 175 to 200 g, Sprague Dawley rats (Charles River, Kent, UK), housed with free access to food and water, under a 12-hour dark/light cycle were used for all in vitro and in vivo experiments. Surgery was performed at the Biomedical Services Unit at the University of Birmingham (Birmingham, UK) in accordance with the Home Office guidelines set out in the 1986 Animal Act (UK) and the ARVO Statement for the Use of Animals in Ophthalmic and Vision Research. All ocular surgical procedures, electrophysiology, and IOP measurements were completed under inhalational anesthesia using 2% to 5% isofluorane/95% O_2 (National Vet Supplies, Stoke, UK) at a flow rate of 1.5L/min. Preoperative 0.1 mg/kg buprenorphine (National Vet Supplies) was administered and the postoperative welfare of all rats was monitored closely.

Experimental Design

At 0 day (0d), one self-sealing incision was made through the cornea into the anterior chamber using a 15° disposable blade enabling repeat twice a week (biweekly) 3.5 μL IC injections through the tunnel generated using self-made disposable sterile glass micropipettes (Harvard Apparatus, Kent, UK) for 30d of either PBS (control group $PBS_{0\text{-}30d}$; Sigma, Poole, UK), active hrTGF-β2 (treatment group TGF-$\beta2_{0\text{-}17d}$ and treatment group TGF-$\beta2_{0\text{-}30d}$; 5 ng/μL; Peprotech, London, UK), active hrTGF-β1 (5 ng/μL; Peprotech) between 0d and 17d then PBS between 21d and 30d (treatment group TGF-$\beta1_{0\text{-}17d}$/$PBS_{21\text{-}30d}$), or active hrTGF-β2 (5 ng/μL) between 0d and 17d then hrDecorin between 21 and 30d (concentration derived from Ahmed et al.[54]; 5 μg/μL; treatment group TGF-$\beta2_{0\text{-}17d}$/$Decorin_{21\text{-}30d}$; Catalent Pharma Solutions, Philadelphia, PA, USA).

Although both TGF-β1 and TGF-β2 were used to raise IOP in this study, experiments with each isoform were analyzed separately and induced similarly raised IOP, fibrosis, and RGC death. Uninjured control eyes (intact) were also analyzed for comparison to the $PBS_{0\text{-}30d}$, TGF-$\beta2_{0\text{-}17d}$, and TGF-$\beta2_{0\text{-}30d}$ groups (Table 1). Intraocular pressure measurements were taken biweekly in all treatment groups timed immediately before the IC injections throughout the 30d experimental period. Visually evoked potentials (VEP) in the $PBS_{0\text{-}30d}$ and TGF-$\beta2_{0\text{-}30d}$ groups were measured at 30d for model validation to assess the functional consequences of RGC death and the tissues from all groups were processed for immunohistochemistry (IHC) to assess levels of TM fibrosis and RGC survival.

IOP Measurements

Using an iCare Tonolab rebound tonometer (Icare, Helsinki, Finland), IOP was recorded biweekly between 9 AM and 11 AM for the duration of each experiment to avoid confounding the readings with circadian variability. Immediately after induction of anaesthesia with 5% Isoflurane, six rebound measurements were taken with the tonometer from the central cornea on each measurement occasion to give an overall average IOP measurement (mm Hg) and all graphical data points represent the mean ± SEM of three readings (of 6 rebounds each) taken sequentially to ensure accurate measurements (as previously described[60]).

Visually Evoked Potentials

To ascertain if the RGC loss caused by the TGF-β–related IOP rise led to functional retinal deficits, VEP measurements were

Table 1. Experimental Design for IC Injections

Experimental Groups		
Intact	n = 4 eyes; control group for $PBS_{0\text{-}30d}$, $TGF\text{-}\beta2_{0\text{-}17d}$ and $TGF\text{-}\beta2_{0\text{-}30d}$	Model validation
$PBS_{0\text{-}30d}$	n = 12 eyes; control group for $TGF\text{-}\beta2_{0\text{-}17d}$ and $TGF\text{-}\beta2_{0\text{-}30d}$	
$TGF\text{-}\beta2_{0\text{-}17d}$	n = 3 eyes; test group for $PBS_{0\text{-}30d}$, control group for $TGF\text{-}\beta2_{0\text{-}30d}$	
$TGF\text{-}\beta2_{0\text{-}30d}$	n = 12 eyes; test group for $PBS_{0\text{-}30d}$, control group for $TGF\text{-}\beta2_{0\text{-}17d}$	
$TGF\text{-}\beta1_{0\text{-}17d}/PBS_{21\text{-}30d}$	n = 6 eyes; control group for $TGF\text{-}\beta2_{0\text{-}17d}/Decorin_{21\text{-}30d}$	Decorin Study
$TGF\text{-}\beta2_{0\text{-}17d}/Decorin_{21\text{-}30d}$	n = 12 eyes; test group for $TGF\text{-}\beta1_{0\text{-}17d}/PBS_{21\text{-}30d}$	

In vivo experimental groups detailing the biweekly IC injection regimes.

compared between the $PBS_{0\text{-}30d}$ and $TGF\text{-}\beta2_{0\text{-}30d}$ treatment groups. Five days before VEP were recorded, the cranial skin was resected and stainless steel screws (Bioanalytical Systems, Inc., Kenilworth, UK) were implanted at 7-mm posterior to the bregma, 3-mm lateral to the midline, at a depth of 0.5 mm into the skull to connect the positive recording electrodes. The reference (negative) screw electrode was inserted into the skull in the midline, 3-mm anterior to bregma. The skin was sutured around the screws. For VEP recordings at 30d, rats were dark-adapted overnight and VEP recorded using an Ocuscience HMsERG rodent ERG machine (Ocuscience, Henderson, NV, USA) in a light-sealed room and prepared under a dim red light. Rats were anaesthetized using 2% isoflurane for the duration of recordings and readings were taken at a controlled 37°C temperature in a Faraday cage to reduce electrical interference. A needle ground electrode was placed in the midline dorsal subcutaneous tissue at the base of the tail. Electrode impedance was maintained below 2 kΩ. A mini-Ganzfeld stimulator was used with increasing stimulus intensities of 300, 3000, and 25,000 mcd/s/m^2, which were averaged 100 times at each intensity with a recording duration of 250 ms and an interstimulus interval of 1 second. Visually evoked potentials from each eye were recorded separately by uniocular occlusion allowing within subject comparison of treatment/injury effects. Visually evoked potentials amplitude and latency was measured in ERGView (Ocuscience) by an observer blinded to the identity of the treatment groups.

Tissue Preparation for Immunohistochemistry

Rats were killed by exposure to increasing concentrations of CO_2 and transcardially perfused with 100 mL of PBS to wash out blood before further perfusion with 100 mL 4% paraformaldehyde (PFA) in PBS at pH 7.4. Dissected eyes for IHC were post fixed by immersion in 4% PFA in PBS for 2 hours at 4°C before cryoprotection by immersion in increasing concentrations of sucrose solutions (PBS with 10%, 20%, and 30% sucrose; all from Sigma) for 24 hours each at 4°C then embedded in optimal cutting temperature (OCT) embedding medium (Thermo Shandon, Runcorn, UK) in peel-away mould containers (Agar Scientific, Essex, UK). Eyes immersed in OCT were rapidly frozen in crushed dry ice before storage at –80°C and later sectioned in the parasagittal plane through the optic nerve head at –22°C using a Bright cryostat microtome (Bright, Huntingdon, UK) at a thickness of 20 μm. Sections were mounted on positively charged glass slides (Superfrost plus; Fisher Scientific, Pittsburgh, PA, USA), left for 2 hours to dry at 37°C and stored at –20°C.

Retinal Cell Culture

Retinal cells were dissociated using a papain dissociation system in accordance with the manufacturer's protocol (Worthington Biochem, Lakewood, NJ, USA) and 120 to 125 $\times 10^3$ cells/well were cultured on sterile glass chamber slides (BD Biosciences, Oxford, UK) precoated with 100 μg/mL poly-D-lysine, followed by 20 μg/mL Laminin-I (both from Sigma) in Neurobasal-A supplemented with B27-supplement, L-glutamine, and penicillin/streptomycin (all from Invitrogen Ltd., Paisley, UK), at 37°C, in a humidified 5% CO_2 atmosphere. After 24 hours in culture, supplemented Neurobasal-A (sNBA) was removed and retinal cells treated with hrDecorin diluted to the test concentrations in fresh sNBA. Wells were treated with 300 μL of either of sNBA (control) or 1, 10, 100, 1000 μg/mL concentrations of hrDecorin in sNBA, and grown for a further 3d, at 37°C, in a humidified 5% CO_2 atmosphere.

Immunocytochemistry

Retinal cultures were fixed in 4% PFA in PBS at room temperature (RT) for 10 minutes, washed 3 × 5 minutes with 0.1% Triton X-100 (Sigma) in PBS and blocked in 0.1% Triton X-100 with 10% normal goat serum (Serotec, Oxfordshire, UK) and 3% bovine serum albumin (BSA; Sigma) in PBS for 30 minutes at RT. Cultures were incubated in mouse anti–βIII-tubulin antibody (1/500; Sigma) for 1 hour at RT. Cultures were then washed 3 × 5 minutes in PBS and incubated in goat anti-mouse IgG Alexa Fluor 488 secondary antibody (1/400; Invitrogen) for 1 hour. After washing in PBS, slides were mounted using Vectamount containing 4′,6-diamidino-2-phenylindole (DAPI; Vector Labs, Peterborough, UK) and viewed using a Zeiss Axioplan2 epi-fluorescent microscope equipped with an AxioCam HRc camera and Axiovision software (all from Carl Zeiss, Hertfordshire, UK). Control tissue sections incubated with secondary antibody alone were all negatively stained (not shown).

Table 2. Antibodies Used in Immunohistochemistry

Antigen	Dilution	Supplier	Catalogue No.	To Identify
Laminin[47]	1:200	Sigma (Poole, UK)	L9393	TM fibrosis
ED1[47]	1:400	Serotec (Kidlington, UK)	MCA341GA	Macrophage
Fibronectin[47]	1:200	Sigma	F3648	TM fibrosis
Human Decorin[47]	1:400	Abcam (Cambridge, UK)	Ab54728	TM fibrosis
MMP2[61]	1:100	Abcam	Ab37150	Pro- and active MMP2 levels
MMP9[61]	1:100	Santa Cruz (Santa Cruz, CA)	SC-10737	Pro- and active MMP9 levels
TIMP2[61]	1:100	Santa Cruz	SC-5539	Pro- and active TIMP2 levels
Brn3a[62]	1:100	Santa Cruz	SC-31984	RGC
Donkey anti-mouse IgG, Alexa Fluor 488	1:400	Molecular Probes (Paisley, UK)	A-21202	Secondary IgG for mouse primary antibodies
Goat anti-mouse IgG Alexa Fluor 594	1:500	Molecular Probes	A-11032	Secondary IgG for mouse primary antibodies
Donkey anti-goat IgG, Alexa Fluor 594	1:400	Molecular Probes	A-11058	Secondary IgG for goat primary antibodies
Donkey anti-rabbit IgG, Alexa Fluor 594	1:400	Molecular Probes	A-21207	Secondary IgG for rabbit primary antibodies
Donkey anti-rabbit IgG, Alexa Fluor 488	1:400	Molecular Probes	A-21206	Secondary IgG for rabbit primary antibodies

Immunohistochemistry

Frozen sections were left to thaw for 30 minutes before 3 × 5 minutes washing in PBS followed by a 20 minutes permeabilization with 0.1% Triton X-100 (Sigma). Nonspecific antibody binding sites in tissue sections were blocked for 30 minutes in 0.5% BSA, 0.3% Tween-20 (all from Sigma), and 15% normal goat serum (Vector Laboratories) in PBS before incubating overnight in primary antibody (Table 2) followed by washing 3 × 5 minutes in PBS and incubating for 1 hour at RT with secondary antibody (Table 2). Sections were then washed 3 × 5 minutes in PBS and mounted in Vectorshield mounting medium containing DAPI (Vector Laboratories). Control tissue sections incubated with secondary antibody alone were all negatively stained (not shown).

Quantification of Immunohistochemistry

After immunofluorescence staining, sections were viewed on a Zeiss Axioplan 2 epi-fluorescent microscope (Carl Zeiss Ltd.) and images captured using the same exposure times (Laminin, fibronectin, and Decorin at 250 ms; MMP2 at 1.2 seconds, MMP9 and TIMP2 at 1 second) for each antibody using a Zeiss AxioCam HRc. Immunohistochemistry staining was quantified according to the methods previously described.[47] Briefly, the region of interest used for quantitation of TM fibrosis was defined by a quadrant of the same prescribed size for all eyes/treatments within the TM. Extracellular matrix deposition was quantified within this defined quadrant of the TM and the percentage of immunofluorescent pixels above a standardized background threshold was calculated using ImageJ software (http://imagej.nih.gov/ij/; provided in the public domain by the National Institutes of Health, Bethesda, MD, USA). For each antibody, the threshold level of brightness in the area of the TM was set using intact untreated eye sections to define the reference level for test group analysis of pixel intensity. Images were assigned randomized numbers to ensure blinding of treatment groups during quantification by the assessor.

For quantification of RGC in retinal sections, $Brn3a^+/DAPI^+$ RGC were counted in 20-μm thick parasagittal sections of retina from a 250-μm linear portion from the ganglion cell layer (GCL) either side of the optic nerve (as previously published[62]). Eight retinal sections from each eye in the control and treatment groups (Table 1) were quantified. Images were assigned randomized numbers to ensure blinding of treatment groups during quantification by the assessor.

For quantification of macrophages, $ED1^+/DAPI^+$ cells were counted in 20-μm thick parasagittal sections of the eye. $ED1^+/DAPI^+$ cell counts were performed in 500 × 400 μm (×20) Axiovision images of the anterior chamber angle (as $ED1^+$ cells were only observed in the angle) of $n = 3$ eyes from intact, $PBS_{0\text{-}30d}$– and TGF-$\beta2_{0\text{-}30d}$–treatment groups. Images were assigned randomized numbers to ensure blinding of treatment groups during quantification by the assessor.

Quantification of RGC in Retinal Cultures

βIII-tubulin$^+$ RGC were counted using Image Pro 6.2 at ×20 magnification in nine equal areas of each well from four random fields of view, totalling 36 images/well. The mean number of βIII-tubulin$^+$ RGC/mm^2 ± SEM was calculated for each image captured within a 0.2475 mm^2 area of each culture well (36 images per well represented $36 \times 0.2475 = 8.91$ mm^2) using previously published methods.[63,64] Retinal ganglion cell counts were performed by an assessor who was blinded to the identity of the treatment groups.

Statistics

All statistical analyses were performed using SPSS 20 (IBM, Chicago, IL, USA). Normal distribution tests were carried out to determine the most appropriate statistical analysis to compare treatments. Statistical significance was determined at P less than 0.05. Intraocular pressure data were analyzed for significant differences using the within-subjects repeated measured design or generalized estimated equations. Trabecular meshwork fibrosis, inflammation, RGC survival, and VEP data were tested for significant differences using Student's t-test or one-way ANOVA for greater than two group comparisons ±SEM and are given in the text or displayed graphically as mean ± SEM. For in vitro RGC survival, between group differences in RGC ± SEM counts were analyzed for significance using ANOVA.

Results

Inflammation Induced by IC Injection

The inflammation induced by repeated IC injection was assessed by counting macrophages/unit area ($ED1^+$ cells) in the angle of eyes from the intact, $PBS_{0\text{-}30d}$ and TGF-$\beta2_{0\text{-}30d}$ groups. The morphology of the eyes remained macroscopically unchanged between intact and treatment groups and there was no evidence of cataracts, hemorrhage, or inflammation in any of the eyes. There was an increase in $ED1^+/DAPI^+$ cells within the iridocorneal angle of eyes that received IC injections of $PBS_{0\text{-}30d}$ and TGF-$\beta2_{0\text{-}30d}$ (9 ± 3 and 12 ± 3 cells, respectively) compared with intact eyes (3 ± 3 cells; $P < 0.001$). However, there were no significant differences in $ED1^+/DAPI^+$ cell

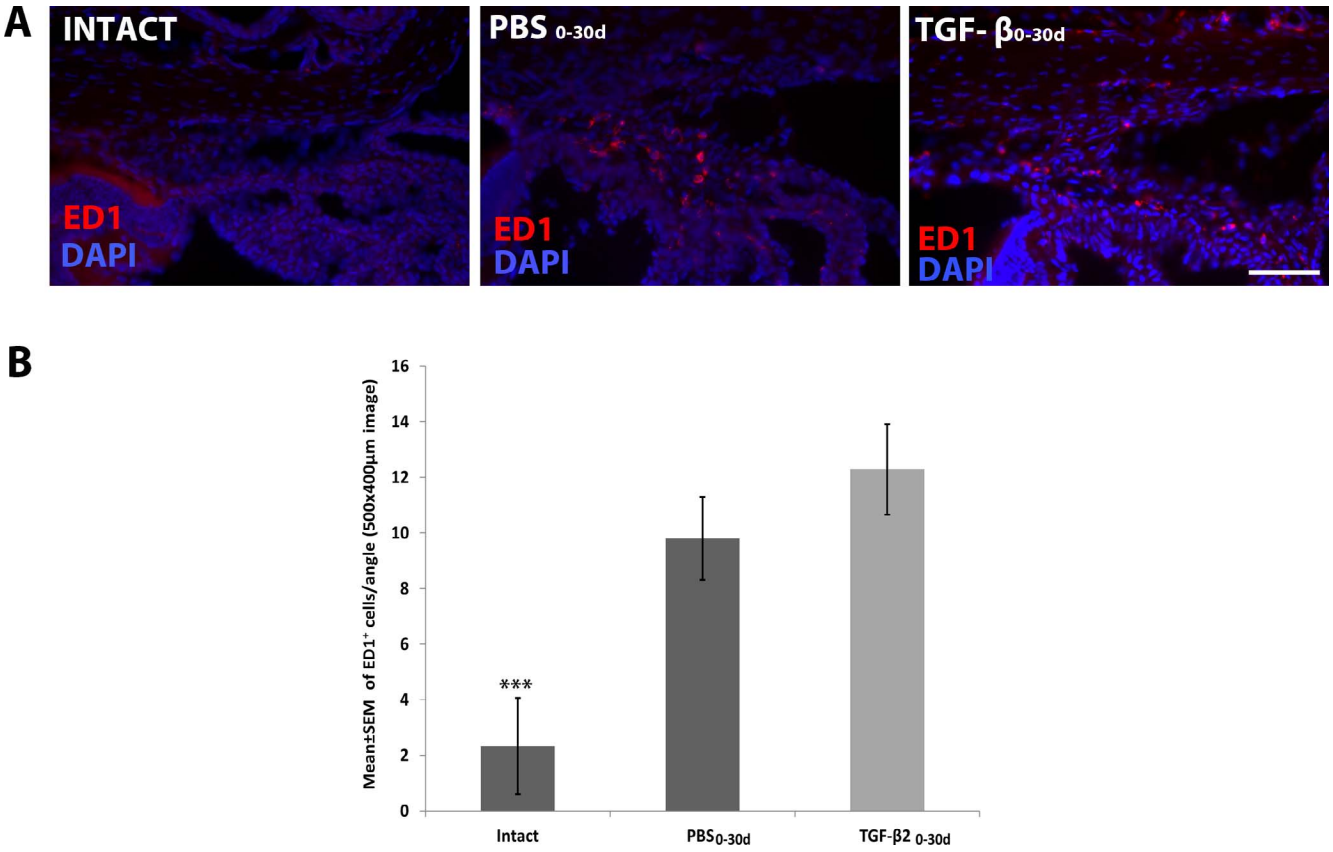

FIGURE 1. Inflammatory response generated from IC injections. The *panels* show parasagittal eye sections illustrating macrophages in the iridocorneal angle. (**A**) ED1 (*red*) and DAPI (*blue*) immunostaining in intact, $PBS_{0\text{-}30d}$, and TGF-$\beta2_{0\text{-}30d}$–treated groups. (**B**) The number of $ED1^+$/$DAPI^+$ cells in the iridocorneal angle. Intact eyes had significantly less $ED1^+$/$DAPI^+$ cells compared with $PBS_{0\text{-}30d}$ and TGF-$\beta2_{0\text{-}30d}$–injected eyes (***$P < 0.001$). *Scale bar*: 100 µm.

counts between the $PBS_{0\text{-}30d}$ and TGF-$\beta2_{0\text{-}30d}$ groups (Fig. 1). The increase in macrophage numbers noted demonstrates that the IC injection caused an inflammatory response within the angle by 30d, with no added effect of TGF-β2.

IC Injections of TGF-β Raises IOP

We evaluated whether IC injection of TGF-β led to the development of TM fibrosis and raised IOP, in order to confirm that our model replicated some of the pathological features of

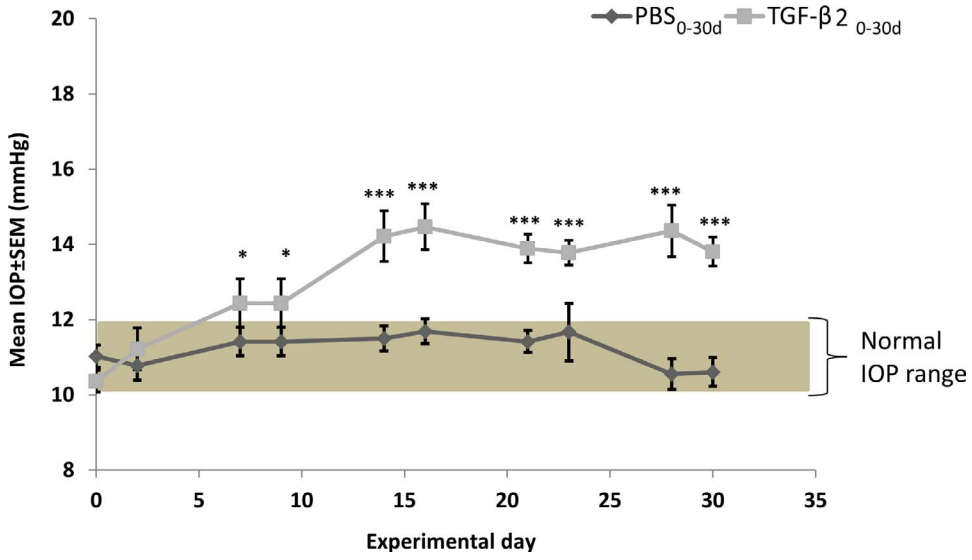

FIGURE 2. Intraocular pressure measurements after biweekly IC TGF-β injections. Tonometer IOP measurements show a significant elevation in IOP by 7d that was sustained through 30d in the eyes of the TGF-$\beta2_{0\text{-}30d}$ group compared with the $PBS_{0\text{-}30d}$ group (*$P < 0.05$ ***$P < 0.001$). The normal IOP range from intact eyes is indicated by the *shaded area*.

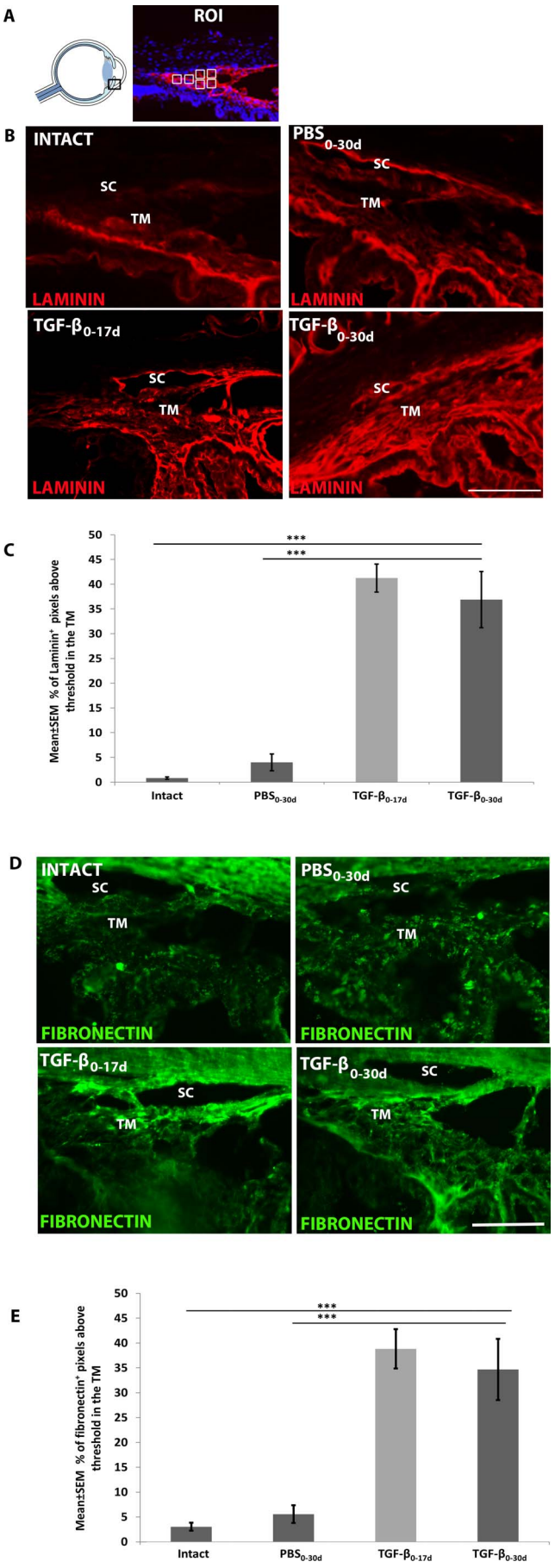

human POAG. Compared with the $PBS_{0\text{-}30d}$ group, IOP increased in the TGF-$\beta2_{0\text{-}30d}$ group, although statistical significance was not achieved until 7d, before which the IOP remained within the normal range of 10.4 ± 0.3 to 12.4 ± 0.7 mm Hg (Fig. 2). From 7d until 30d, IOP increased and was maintained at a significantly higher level of 14 ± 0.3 mm Hg at 30d in the TGF-$\beta2_{0\text{-}30d}$–treated group ($P < 0.05$ at 7–14d; $P < 0.001$ between 14–30d) when compared with IOP in the $PBS_{0\text{-}30d}$ group, which remained within the normal range of 10.5 ± 0.4 to 11.7 ± 0.3 mm Hg throughout. The sustained increase in IOP demonstrates that TGF-β is a suitable agent to induce increased IOP by IC injection in rats.

IC Injections of TGF-β Induces TM Fibrosis

In the control Intact and $PBS_{0\text{-}30d}$ groups, the ciliary body, iris, and vascular basement membranes were all laminin$^+$, particularly around the outer wall of Schlemm's Canal, although laminin$^+$ immunoreactivity was thin along the inner wall (not shown). Thin linear strands of laminin$^+$ tissue were also present within the TM of the intact and $PBS_{0\text{-}30d}$ control groups, while increased laminin$^+$ immunoreactivity was observed in and about the TM of the TGF-$\beta2_{0\text{-}17d}$ and TGF-$\beta2_{0\text{-}30d}$ groups compared with levels in the $PBS_{0\text{-}30d}$ control group ($P < 0.001$; Figs. 3A, 3B, 3C). There were no significant differences in laminin levels between the TGF-$\beta2_{0\text{-}17d}$ and TGF-$\beta2_{0\text{-}30d}$ groups. In both TGF-β groups, laminin immunoreactivity was also particularly prominent in the inner wall of Schlemm's canal.

At 17d and 30d, the TM was also densely packed with fibronectin deposits in the TGF-$\beta2_{0\text{-}30d}$ group, unlike the Intact and $PBS_{0\text{-}30d}$ control groups where little or no fibronectin deposits were observed (Fig. 3D), so that fibronectin levels around the TM were significantly higher in the TGF-$\beta2_{0\text{-}17d}$ and TGF-$\beta2_{0\text{-}30d}$ groups compared with the TM of the $PBS_{0\text{-}30d}$ control group ($P < 0.001$; Fig. 3E). There were no significant differences in fibronectin levels between the TGF-$\beta2_{0\text{-}17d}$ and TGF-$\beta2_{0\text{-}30d}$ groups. These findings demonstrate that IC injections of TGF-β caused excess ECM deposition within and around the TM and Schlemm's Canal and that the ECM deposition occurred by 17d and was maintained at similar levels through to 30d.

TGF-β Induced Fibrosis and Raised IOP Is Associated With RGC Death and Perturbed Retinal Function

Compared with the intact control group (Fig. 4A), Brn3a$^+$ RGC counts from the $PBS_{0\text{-}30d}$- (Fig. 4B), and TGF-$\beta2_{0\text{-}17d}$– (Fig. 4C) treated groups were not significantly different. However, when

Figure 3. Trabecular meshwork fibrosis in the iridocorneal angle. The *panels* show parasagittal eye sections illustrating: (**A**) the region of interest example of quantified areas in the TM (*white boxes*) and laminin (*red*) DAPI (*blue*) for illustrative purposes; (**B**) laminin (*red*) immunostaining in intact and $PBS_{0\text{-}30d}$ control groups and also in TGF-$\beta2_{0\text{-}17d}$– and TGF-$\beta2_{0\text{-}30d}$–treated groups. (**C**) Quantification of the percentage laminin$^+$ pixels in a defined area within the TM demonstrating significantly increased laminin immunoreactivity in the TGF-$\beta2_{0\text{-}17d}$– and TGF-$\beta2_{0\text{-}30d}$–treated groups ($P < 0.001$) compared with intact and $PBS_{0\text{-}30d}$ controls. (**D**) Fibronectin (*green*) immunostaining in the TM of intact and $PBS_{0\text{-}30d}$ control groups and also in TGF-$\beta2_{0\text{-}17d}$– and TGF-$\beta2_{0\text{-}30d}$–treated groups. (**E**) Quantification of the percentage fibronectin$^+$ pixels in a defined area within the TM demonstrating significantly increased fibronectin immunoreactivity in the TGF-$\beta2_{0\text{-}17d}$– and TGF-$\beta2_{0\text{-}30d}$–treated groups (***$P < 0.001$) compared with intact and $PBS_{0\text{-}30d}$ controls. *Scale bar*: 100 μm; SC, Schlemm's Canal.

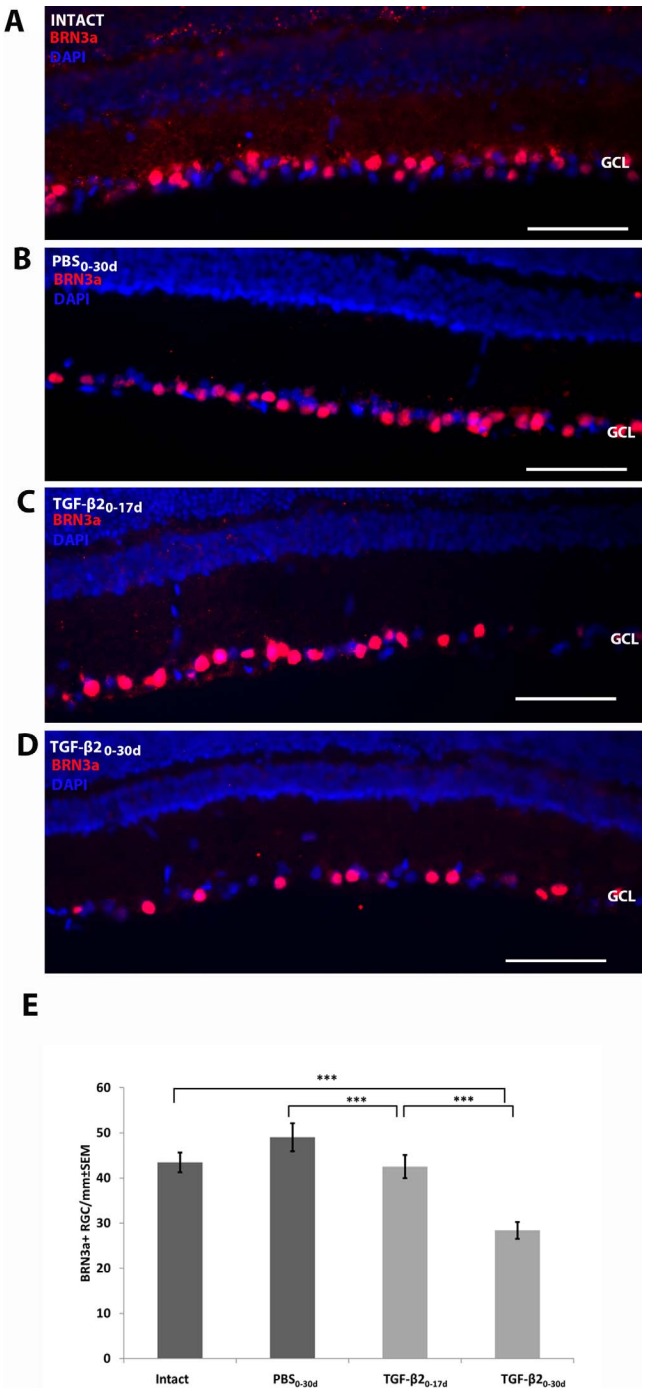

FIGURE 4. BRN3a$^+$ RGC counts in the GCL. The *panels* show: (**A**) Brn3a$^+$(*red*)/DAPI$^+$(*blue*) RGC in parasagittal retinal sections from the intact control group. (**B**) Brn3a$^+$/DAPI$^+$ RGC in the PBS$_{0\text{-}30d}$ control group. (**C**) Brn3a$^+$/DAPI$^+$ RGC in the TGF-β2$_{0\text{-}17d}$–treated group. (**D**) Brn3a$^+$/DAPI$^+$ RGC in TGF-β2$_{0\text{-}30d}$–treated group. (**E**) Quantification of Brn3a$^+$/DAPI$^+$ RGC survival in the intact and PBS$_{0\text{-}30d}$ control groups and also in the TGF-β2$_{0\text{-}17d}$– and TGF-β2$_{0\text{-}30d}$–treated groups. IC TGF-β2$_{0\text{-}30d}$ was associated with significantly higher levels of RGC death when compared with intact, PBS$_{0\text{-}30d}$ and TGF-β2$_{0\text{-}17d}$ groups (***$P <$ 0.001). *Scale bar*: 100 μm.

compared with the counts in the intact (43 ± 2 RGC/mm) and the PBS$_{0\text{-}30d}$ (49 ± 2 RGC/mm) control group retinae, RGC counts from the TGF-β$_{0\text{-}30d}$–treated group (Fig. 4D) were lowered (28 ± 3 RGC/mm, $P < 0.001$), indicating statistically significant RGC death (Fig. 4E). The Brn3a$^+$ RGC counts in the TGF-β2$_{0\text{-}17d}$–treated group were higher than those in the TGF-β2$_{0\text{-}30d}$–treated group and not significantly different from RGC numbers in control intact and PBS$_{0\text{-}30d}$ groups, suggesting that most of the RGC loss occurred between 17d and 30d.

The RGC loss was associated with a significant decrease in the P1/N2 VEP amplitude in the TGF-β2$_{0\text{-}30d}$–treated group when compared with the control PBS$_{0\text{-}30d}$ group ($P < 0.01$; Figs. 5A, B), but there was no change in P1/N2 latency ($P > 0.05$).

hrDecorin Attenuates TGF-β–Induced IOP Elevation

We next investigated whether IC hrDecorin delivered over the 21d to 30d period attenuated the IOP elevation and TM fibrosis established by IC TGF-β injections delivered between 0d and 17d, as well as the effects of hrDecorin on RGC survival. Having caused a sustained elevation in IOP through repeated IC TGF-β2 injections over 17d, administration of hrDecorin between 21d and 30d significantly and contemporaneously decreased IOP to control levels ($P < 0.001$; Fig. 6). Accordingly, the IOP in the TGF-β2$_{0\text{-}17d}$/Decorin$_{21\text{-}30d}$ group was still at 15 ± 2 mm Hg at 21d, indistinguishable from IOP in the TGF-β1$_{0\text{-}17d}$/PBS$_{21\text{-}30d}$ group at 14 ± 2 mm Hg. However, by 30d the IOP in the TGF-β2$_{0\text{-}17d}$/Decorin$_{21\text{-}30d}$ group had significantly lowered to 10 ± 0.6 mm Hg compared with an IOP of 16 ± 1 mm Hg in the TGF-β1$_{0\text{-}17d}$/PBS$_{21\text{-}30d}$ group at 30d. Hence, hrDecorin delivered between 21d and 30d reduced IOP to levels similar to values recorded in the Intact and the PBS$_{0\text{-}30d}$ control groups by 30d.

hrDecorin Causes the Dissolution of Established TM Fibrosis

In the TGF-β2$_{0\text{-}17d}$/Decorin$_{21\text{-}30d}$ group, laminin and fibronectin deposits were significantly reduced at 30d ($P < 0.05$; Fig. 7A–D) throughout the TM compared with those in the TGF-β1$_{0\text{-}17d}$/PBS$_{21\text{-}30d}$ and TGF-β2$_{0\text{-}17d}$ control groups (Fig. 7). Laminin immunoreactivity in the TGF-β1$_{0\text{-}17d}$/PBS$_{21\text{-}30d}$ control group was observed most prominently throughout the inner wall of Schlemm's Canal, while fibronectin was deposited throughout the TM but was most prominent within the JCT region. However, the TGF-β2$_{0\text{-}17d}$/Decorin$_{21\text{-}30d}$ regime significantly ($P < 0.001$) reduced these deposits, giving a similar pattern of laminin and fibronectin staining to that observed in the PBS$_{0\text{-}30d}$ and intact control groups. The decrease in laminin and fibronectin deposits in the TM shown by immunohistochemistry, together with the lowered IOP, suggests that injections of hrDecorin over the period of 21d to 30d caused the dissolution of established fibrosis induced by IC TGF-β injections over the 0d to 17d period.

hrDecorin Induces Fibrolysis of TM ECM by Increasing the MMP/TIMP Ratio

We next investigated whether hrDecorin modulated lysis of TGF-β-induced TM fibrosis through modulation of the MMP axis. Immunostaining was undertaken to localize hrDecorin in the TM at 30d (Figs. 8A, 8E). In the PBS$_{0\text{-}30d}$ and TGF-β1$_{0\text{-}17d}$/PBS$_{21\text{-}30d}$ control groups, little hrDecorin$^+$ immunoreactivity was observed. By contrast, levels of hrDecorin in the TGF-β2$_{0\text{-}17d}$/Decorin$_{21\text{-}30d}$ group were significantly higher within the TM compared with the PBS$_{0\text{-}30d}$ and TGF-β1$_{0\text{-}17d}$/PBS$_{21\text{-}30d}$ control groups ($P < 0.001$), reflecting the local accumulation of injected hrDecorin in the TGF-β2$_{0\text{-}17d}$/Decorin$_{21\text{-}30d}$ group (Fig. 8E). The constitutive levels of total MMP2 staining in the TM seen in the control PBS$_{0\text{-}30d}$ group (Figs. 8B, E) and the intact group (not shown) were suppressed in the TGF-β1$_{0\text{-}17d}$/PBS$_{21\text{-}30d}$ group, an

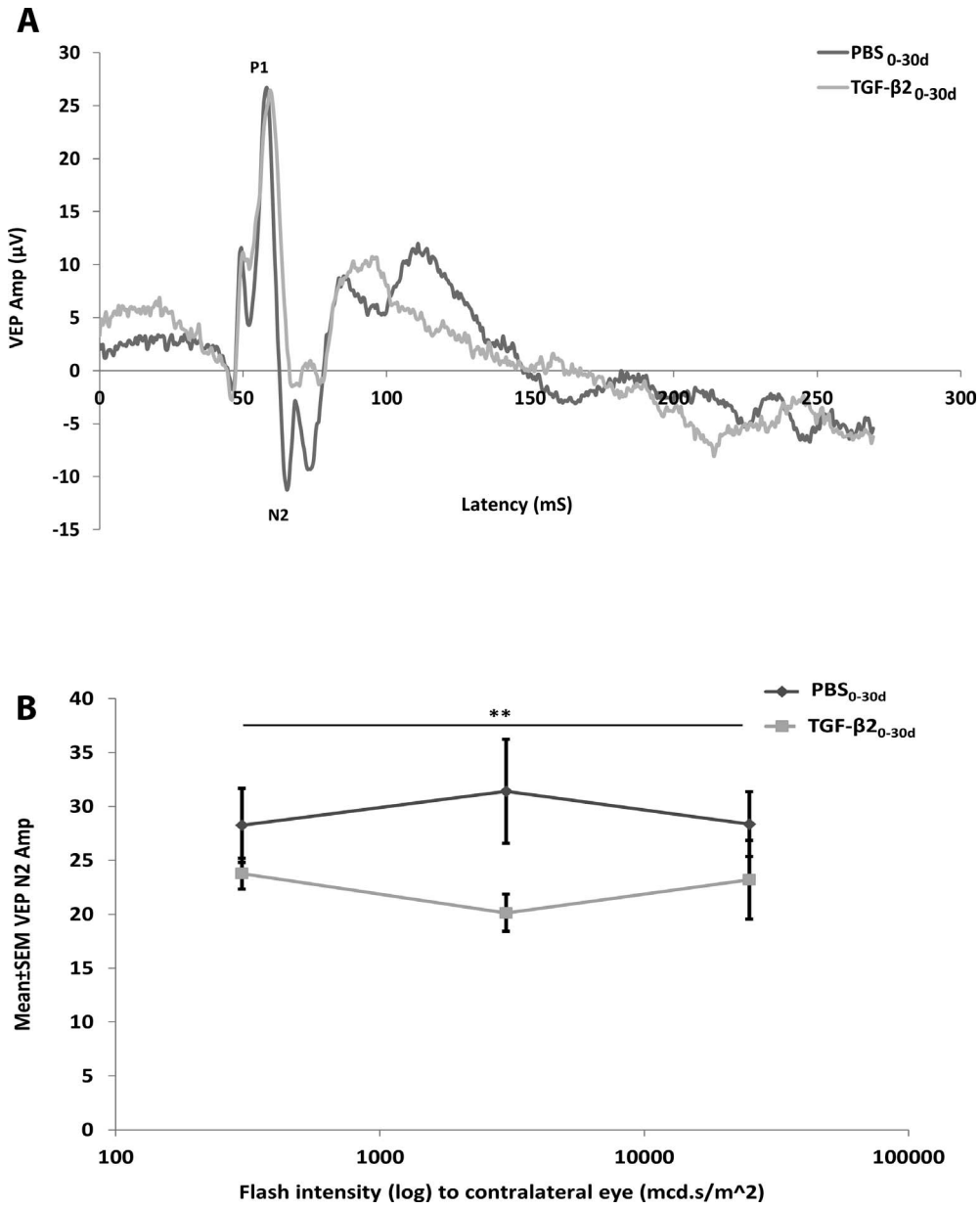

Figure 5. Functional assessment of the visual pathway using flash VEP. (**A**) Representative VEP recordings at flash intensity of 3000 mcd.s/m^2 showing a decrease in wave amplitude in the TGF-$\beta2_{0\text{-}30d}$–treated group compared to the $PBS_{0\text{-}30d}$ control group. (**B**) Average VEP amplitude at P1/N2 in the $PBS_{0\text{-}30d}$ and the TGF-$\beta2_{0\text{-}30d}$ groups. There was a significant reduction in wave amplitude at P1/N2 in the TGF-$\beta2_{0\text{-}30d}$–treated group compared with the $PBS_{0\text{-}30d}$ control group ($n = 8$ eyes/group $^{**}P < 0.01$).

effect that was neutralized by TGF-$\beta2_{0\text{-}17d}$/$Decorin_{21\text{-}30d}$ treatment, increasing levels of MMP2 to those seen in the $PBS_{0\text{-}30d}$ group (Figs. 8B, 8E). Similarly, the TM of the TGF-$\beta1_{0\text{-}17d}$/$PBS_{21\text{-}30d}$ group had significantly lower levels of immunoreactive MMP9 than did the $PBS_{0\text{-}30d}$ and TGF-$\beta2_{0\text{-}17d}$/$Decorin_{21\text{-}30d}$ groups (Figs. 8C, 8E). Conversely, TIMP2 immunoreactivity was similar in both $PBS_{0\text{-}30d}$ and TGF-$\beta1_{0\text{-}17d}$/$PBS_{21\text{-}30d}$ groups, but was significantly lowered in the TGF-$\beta2_{0\text{-}17d}$/$Decorin_{21\text{-}30d}$ group (Figs. 8D, 8E). Quantitation of the immunoreactivity confirmed these changes in the TGF-$\beta2_{0\text{-}17d}$/$Decorin_{21\text{-}30d}$ group, so that there was a significant ($P < 0.05$) increase of the MMP2/9:TIMP2 ratio in the TM, favoring MMP activation (Table 3). Thus, TGF-β suppressed MMP2/9 activation in the TM favoring fibrogenesis and hrDecorin reversed this effect, suggesting a mechanism for hrDecorin-mediated lysis of established TM fibrosis.

hrDecorin Treatment Is Indirectly RGC Neuroprotective

In the TGF-$\beta2_{0\text{-}17d}$/$Decorin_{21\text{-}30d}$ group there were significantly higher numbers of surviving RGC at 30d compared with the TGF-$\beta1_{0\text{-}17d}$/$PBS_{21\text{-}30d}$ control group, with 41 ± 4 RGC/mm and 27 ± 2 RGC/mm, respectively ($P < 0.001$; Figs. 9A–C), demonstrating that IC hrDecorin attenuated RGC loss between 21d and 30d as observed in Figure 4D. To assess whether this reflected a direct or indirect effect of hrDecorin on RGC, the neuroprotective effects were tested in vitro. Treatment of

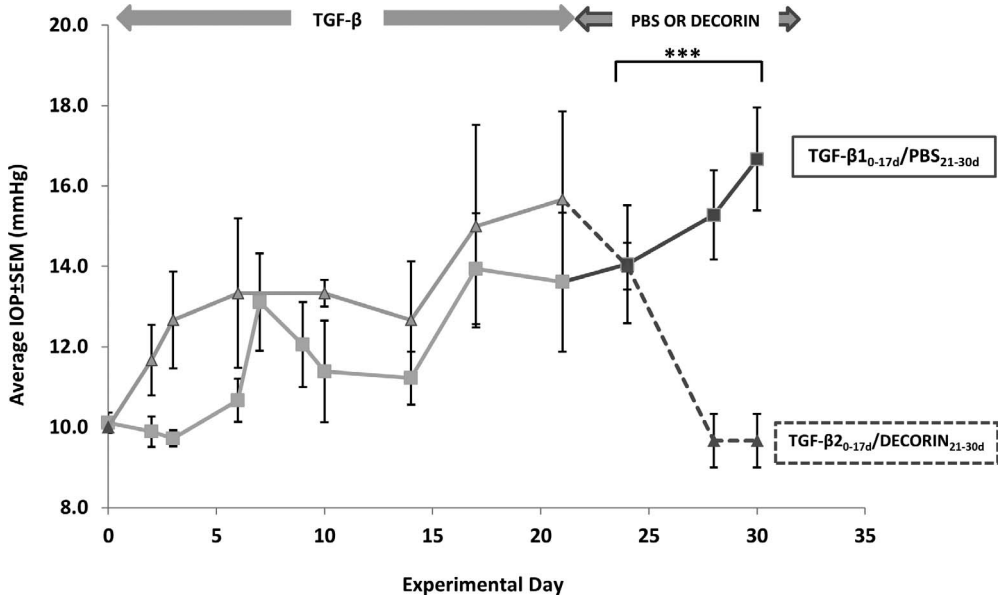

FIGURE 6. Intraocular pressure measurements after IC injection of TGF-β2$_{0-17d}$/Decorin$_{21-30d}$ and TGF-β1$_{0-17d}$/PBS$_{21-30d}$. The graph shows that the sustained elevation in IOP induced by 17d of TGF-β IC injections was reversed by subsequent IC Decorin injections in the TGF-β2$_{0-17d}$/Decorin$_{21-30d}$ group. Intraocular pressure in the TGF-β1$_{0-17d}$/PBS$_{21-30d}$ control group continued to rise beyond 17d when IC TGF-β injections were stopped and replaced by PBS injections (***$P < 0.001$).

retinal cell cultures with increasing concentrations of exogenous hrDecorin did not significantly change the β-III tubulin$^+$ RGC frequency in any of the Decorin treatment groups (1, 10, 100, or 1000 μg/mL) compared with controls ($P = 0.849$). Thus, there was no direct neuroprotective effect of hrDecorin on RGC apparent in vitro (Fig. 9D), implying that the RGC protection observed in vivo was indirect and a consequence of hrDecorin-mediated IOP reduction.

DISCUSSION

Repeated IC injection of TGF-β in adult rats induced TM fibrosis and elevated IOP leading to RGC death and retinal dysfunction, shown by IHC, IOP measurements, RGC counts, and VEP recordings. We have demonstrated that IC hrDecorin treatment decreased fibrosis established by IC TGF-β within the TM (an effect accompanied by increased local levels of MMP2 and MMP9 and reduced levels of TIMP2 implying increased fibrolysis), lowered the raised IOP and, by lowering IOP, indirectly protected the retina from progressive RGC death.

Consistent with other fibrotic models of raised IOP,[20,22] our rodent model of IC TGF-β injections generated a sustained and significant increase in IOP by 14d compared with controls. The baseline level of IOP (before any treatment) reported in the rat by Robertson et al.[20] is similar to that seen in our study. However, overexpression of TGF-β by gene transfer in the Robertson et al.[20] study led to sustained IOP elevations of greater than 20 mm Hg at 14d, higher than our recordings of greater than 14 mm Hg at 14d, probably explained by the constant production of TGF-β through gene transcription compared with our discontinuous bolus regime of biweekly IC injections. Nevertheless, our protocol did cause TM fibrosis accompanied by a sustained rise in IOP, significant RGC loss and retinal dysfunction. An advantage of our model is that TGF-β treatment could be stopped at 17d to reveal that by this time point the IOP was elevated, probably through established TM fibrosis and perturbed AqH drainage. It could be argued that the cessation of TGF-β treatment once fibrosis was established in our model would, over longer time periods, lead to a natural resolution of fibrosis and IOP (due to continued ECM turnover in the TM). However, such resolution was not apparent in the TGF-β1$_{0-17d}$/PBS$_{21-30d}$ treatment group.

We found that raised levels of TGF-β in the AqH induced a robust amount of TM fibrosis. Trabecular meshwork cells contain a high density of TGF-β receptors, making the TM particularly sensitive to raised levels of AqH TGF-β1/TGF-β2.[15,27,31] Binding to a common receptor, TGF-β1/TGF-β2 activates a common intracellular Smad signaling pathway in TM cells, increasing synthesis and local accumulation of ECM proteins, as well as suppressing local ECM protease activity by downregulating MMP,[14] resulting in increased TM fibrosis and enhanced resistance to AqH outflow. In our study, TGF-β–induced TM fibrosis led to an increase in IOP by 17d that was sustained through to 30d and was associated with 42% RGC death at 30d. The functional VEP deficits seen at 30d validate the retinal effects of our TM fibrotic model and are consistent with VEP deficits seen in other experimental models of raised IOP.[65]

Another important factor to consider in our model was the inflammation caused by repeated IC injections. In our study inflammation was measured by counting the number of ED1$^+$ macrophages found in the iridocorneal angle. Our results showed that IC injections increased the number of macrophages in the angle compared with numbers in the intact control eyes, but there were no differences in macrophage numbers between the PBS$_{0-30d}$ and TGF-β2$_{0-30d}$ groups. In light of this, we concluded that any measured differences seen between the two treatments were a consequence of differences in the effects of the delivered agents and were not due to inflammatory effects related to the surgical procedure.

Decorin is naturally found as part of the TM ECM and its presence here is essential to maintain the integrity of the AqH outflow system under normal physiology. However, Decorin also regulates many signalling pathways associated with TM pathologies (e.g., by sequestering TGF-β and inhibiting its associated signalling through Smad2 and Smad3 pathways),[47,48] thereby preventing TM cells from becoming

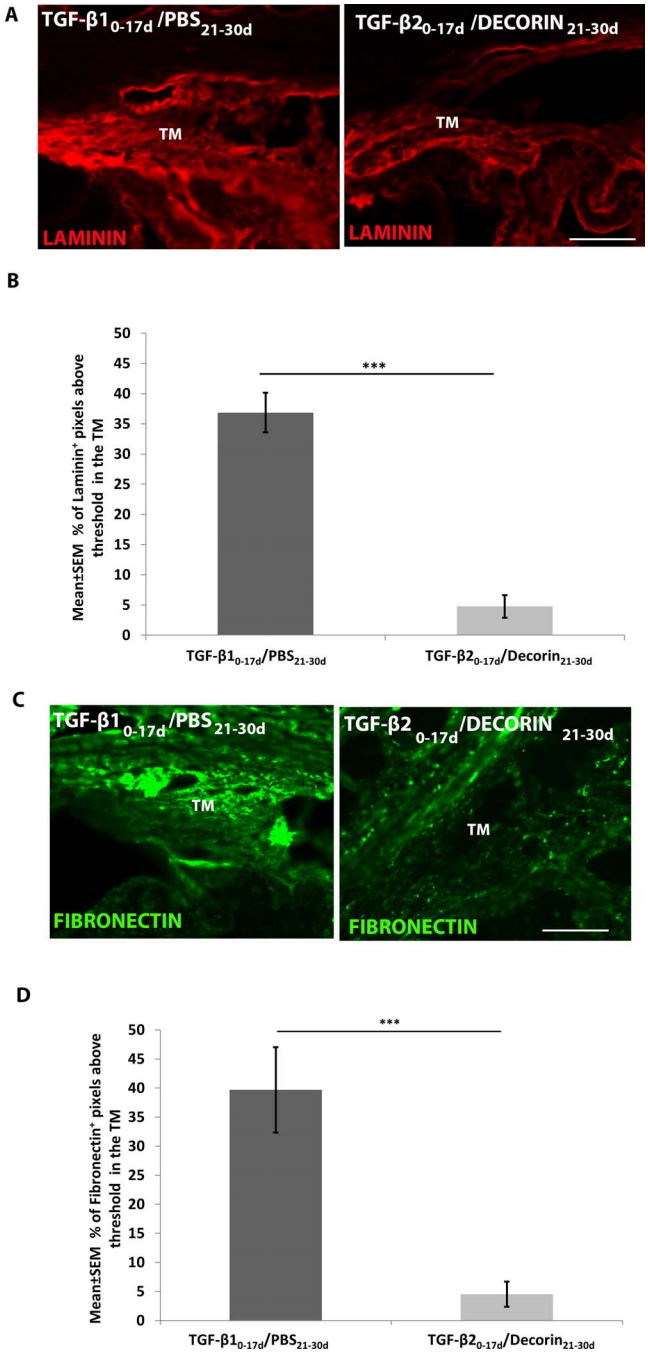

FIGURE 7. Fibrosis in the TM with and without Decorin treatment after sustained IOP elevation induced by IC TGF-β injections. The *panels* show parasagittal eye sections illustrating areas of fibrosis in the angle containing the TM and Schlemm's canal revealed by (**A**) immunostaining of laminin (*red*) and (**B**) quantitation of the laminin immunostaining within a defined region of the TM. (**C**) Immunostaining for fibronectin (*green*) and (**D**) quantitation of the fibronectin immunostaining within a defined region of the TM. The excess deposition of laminin and fibronectin about the TM, induced by IC TGF-$\beta1_{0\text{-}17d}$/$PBS_{21\text{-}30d}$ treatment, was significantly reversed by Decorin treatment in the TGF-$\beta2_{0\text{-}17d}$/$Decorin_{21\text{-}30d}$–treated group (***$P < 0.001$). *Scale bar*: 100 μm.

fibroblast-like and depositing ECM. In addition, Decorin sequesters other growth factors, including IGF-1,[52] EGF,[50] platelet-derived growth factor (PDGF),[66] and VEGF,[51] and interferes with related receptors, as well as directly binding to collagen to alter fibrillogenesis.[53] The direct dissolution of ECM by Decorin-induced MMPs, is also well documented.[55,67] In addition to the Decorin-induced reduction of laminin and fibronectin in the scarred TM, we demonstrated that Decorin altered MMP/TIMP ratios in the TM that were favorable to TM fibrolysis, which probably accounted for the dissolution of established ECM protein deposits in and around the TM. Multiple rodent central nervous system injury models have also demonstrated similar antifibrogenic and fibrolytic actions of Decorin in pathological scenarios of both acute and chronic scarring.[55,59,67]

TABLE 3. MMP:TIMP Ratio After $PBS_{0\text{-}30d}$, TGF-$\beta1_{0\text{-}17d}$/$PBS_{21\text{-}30d}$, and TGF-$\beta2_{0\text{-}17d}$/$Decorin_{21\text{-}30d}$ Treatments

	PBS $_{0\text{-}30d}$	TGF-$\beta_{0\text{-}17d}$/ $PBS_{21\text{-}30d}$	TGF-$\beta_{0\text{-}17d}$/ $Decorin_{21\text{-}30d}$
MMP2:TIMP2	1.33	0.81	4.66
MMP9:TIMP2	1.33	0.85	6.16

Others have shown that Decorin lowers IOP through attenuation of conjunctival scarring in a rabbit model of glaucoma filtration surgery,[68] supporting our observation of reduced IOP through antifibrotic effects of Decorin in the TM. Sequential staging of the injections of TGF-β and Decorin injections in the TGF-$\beta_{0\text{-}17d}$/$Decorin_{21\text{-}30d}$ group exclude the possibility of direct antagonism of exogenously delivered TGF-β by Decorin, implying that the IOP reduction observed with Decorin treatment was not related to direct antagonism of TGF-β, but was a consequence of lysis of the established TM fibrosis, probably by activation of locally produced fibrolytic MMP and coincident inactivation of TIMP.

It is becoming widely accepted that dysfunctional ECM remodelling leads to TM fibrosis in open angle glaucoma (Maatta M, et al. *IOVS* 2002;43:ARVO E-Abstract 2458 and Refs. 69–71). We believe that the rise in IOP seen by 14d and sustained through 30d in this study was due to the development of TM scarring over this period, a contention supported by the fibrosis data shown in both the TGF-$\beta_{0\text{-}17d}$ and TGF-$\beta_{0\text{-}17d}$/$PBS_{21\text{-}30d}$ groups. The rebalancing of MMP:TIMP ratios toward fibrolytic activity mediated by Decorin[54] treatment is mirrored by the pathology of POAG in which MMPs, released from the TM cells, regulate AqH outflow resistance by modulating ECM turnover in the TM.[72,73] Studies that involve stretching of TM cells by eye perfusion have shown that increased IOP leads to upregulated levels of MMP2 and downregulated TIMP2 levels, thus favoring ECM degradation with consequent lowering of IOP.[72] In the present study, Decorin treatment similarly reversed established TM fibrosis, making Decorin a candidate drug to reverse the pathology of ocular hypertension and various forms of open-angle glaucoma.

Although Decorin treatment lowered IOP and increased RGC survival compared with controls in vivo, our in vitro study demonstrated that Decorin was not directly RGC neuroprotective. Seidler et al.[74] reported an antiapoptotic effect of Decorin in cultured fibroblasts by prevention of DNA fragmentation. Others have also shown that Decorin promotes survival of endothelial and epithelial cells[49,75] but conversely, there is a body of literature from cancer cell studies that convincingly demonstrates the ability of Decorin to induce apoptosis,[76–78] so cell context is seemingly important to Decorin actions. Given that, in our primary retinal cultures Decorin did not demonstrate any significant RGC survival, we infer that the Decorin-related neuroprotection observed in vivo was probably indirect and attributable to the IOP-lowering effects that reflected restoration of normal AqH outflow as a

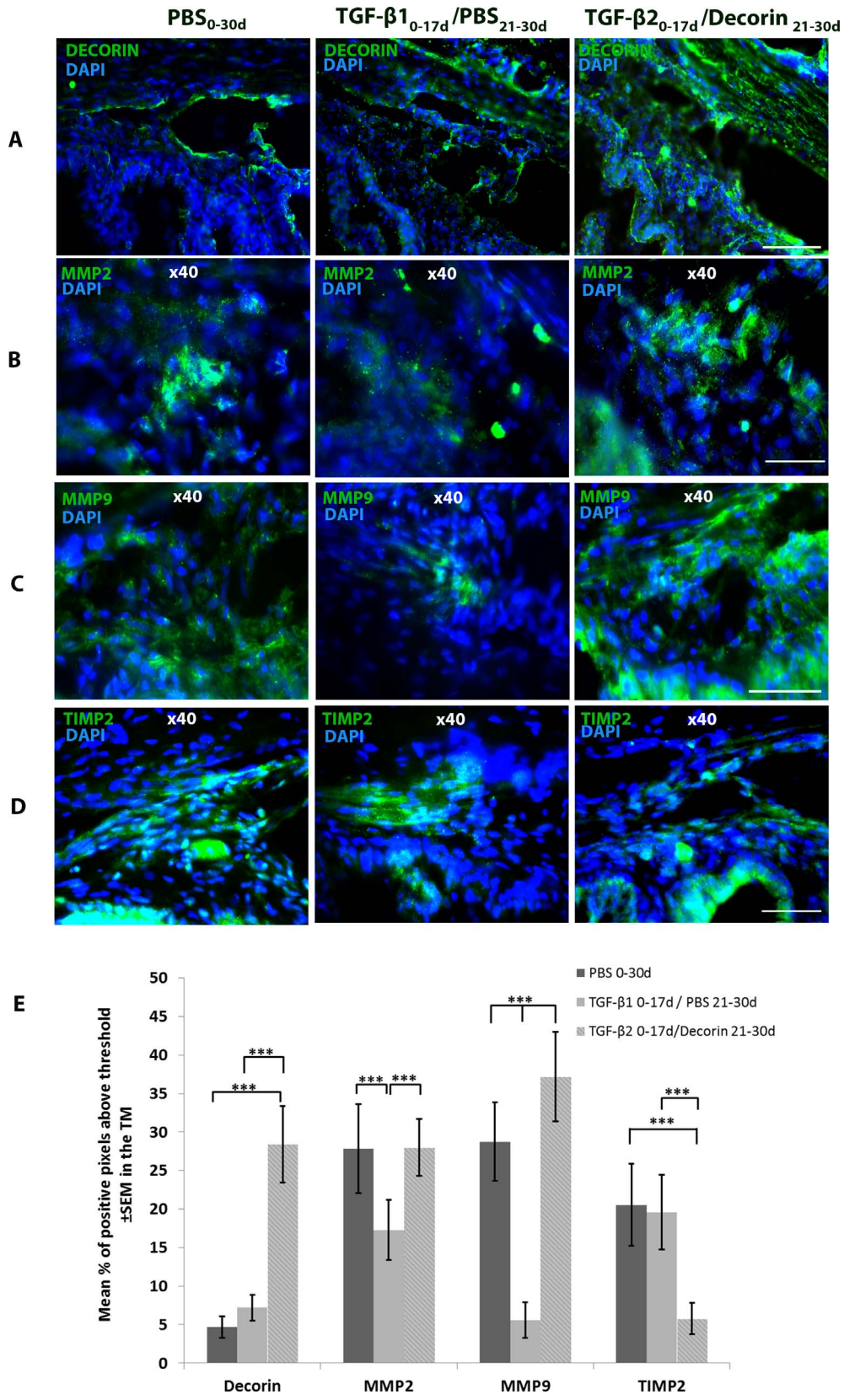

Figure 8. Decorin and protease levels in the TM. *Panels* show representative images of immunoreactive (*green*). (**A**) Decorin in the angle, (**B**) total MMP2, (**C**) total MMP9, and (**D**) total TIMP2 within the TM of the $PBS_{0\text{-}30d}$ and TGF-$\beta1_{0\text{-}17d}$/$PBS_{21\text{-}30d}$ control groups and in the TGF-$\beta2_{0\text{-}17d}$/$Decorin_{21\text{-}30d}$–treated groups, with (**E**) quantification of pixel intensities above the threshold from a defined region within the TM that was set in Intact control eyes. The data demonstrate that in the TGF-$\beta_{0\text{-}17d}$/$Decorin_{21\text{-}30d}$–treated group there was increased levels of both MMPs and decreased levels of TIMP2 in the TM tissues (***$P < 0.001$); *Scale bar*: 100 μm for (**A**) and 50 μm for (**B**–**D**).

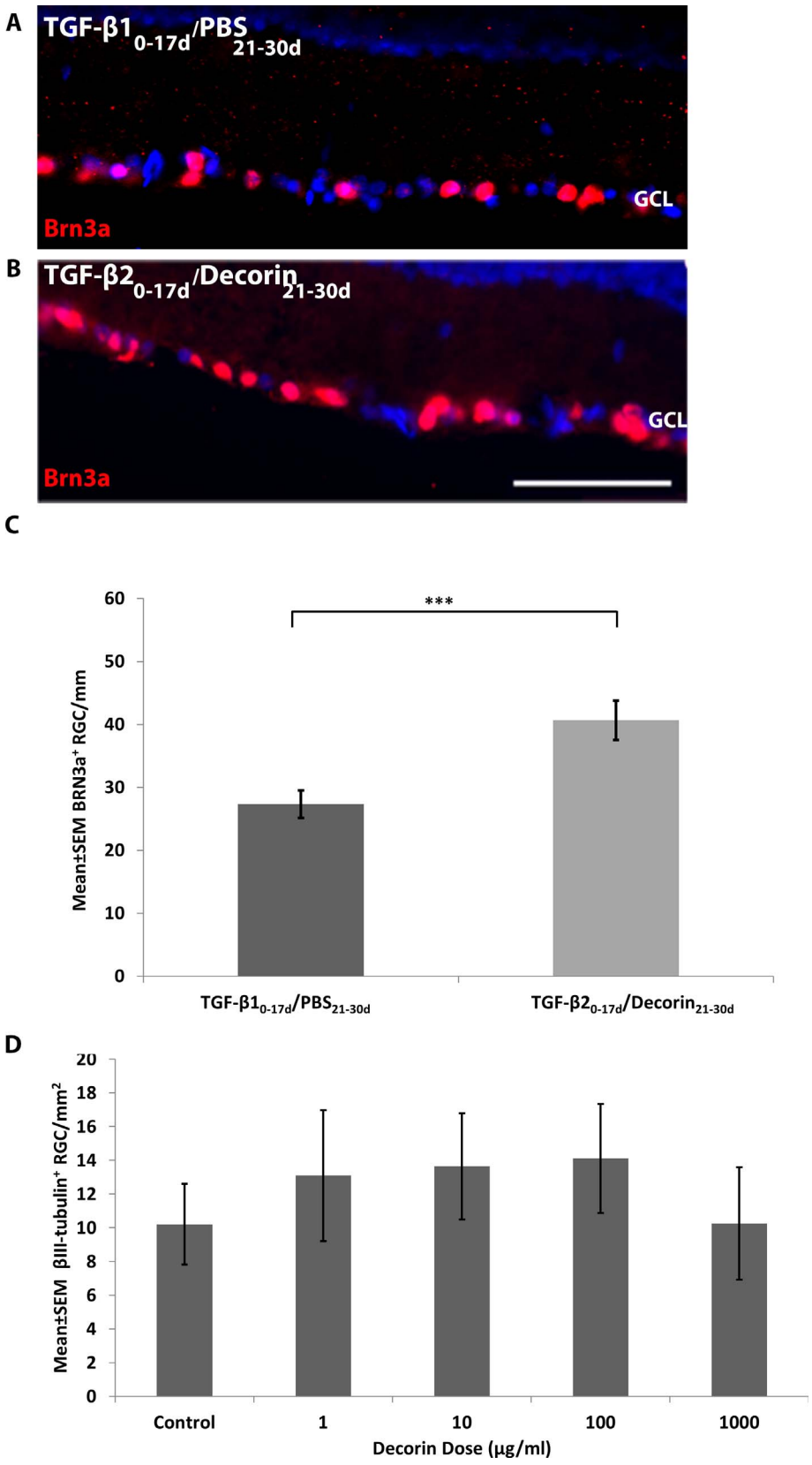

Figure 9. In vivo and in vitro RGC survival after Decorin treatment. The *panels* illustrate $Brn3a^+/DAPI^+$ staining in the GCL of the (**A**) TGF-$\beta1_{0\text{-}17d}$/$PBS_{21\text{-}30d}$–treated group and (**B**) TGF-$\beta2_{0\text{-}17d}$/$Decorin_{21\text{-}30d}$–treated group. The *graphs* show quantitation of RGC survival (**C**) in vivo in the TGF-$\beta1_{0\text{-}17d}$/$PBS_{21\text{-}30d}$–treated and the TGF-$\beta2_{0\text{-}17d}$/$Decorin_{21\text{-}30d}$–treated groups and (**D**) in vitro after retinal cell culture with various concentrations of Decorin. Retinal ganglion cell death was significantly reduced in the TGF-$\beta2_{0\text{-}17d}$/$Decorin_{21\text{-}30d}$ group compared with the TGF-$\beta1_{0\text{-}17d}$/$PBS_{21\text{-}30d}$ group (***$P < 0.001$; *Scale bar*: 100 μm). However, there was no significant direct neuroprotective effect of Decorin on RGC in vitro.

consequence of MMP-induced dissolution of TM fibrosis. Currently, there is no precise explanation of why high IOP causes RGC death, a multitude of factors may contribute, including compromised retrograde axonal transport of target-derived neurotrophic factors, activation of apoptosis and mitochondrial dysfunction after biomechanical and ischemic insults caused by compression of the optic nerve head as a result of raised IOP.[79]

In conclusion, our observations suggest that IC Decorin effectively reversed established TM fibrosis and normalized IOP, thereby indirectly protecting RGC from progressive IOP-related death. Thus, Decorin has the potential to be developed into an effective therapy for patients with ocular hypertension and forms of open-angle glaucoma associated with TM fibrosis.

Acknowledgments

The authors thank Hannah Botfield, Simon Foale, and Adam Thompson from the University of Birmingham for their technical assistance. They also thank Catalent Pharma Solutions (Philadelphia, PA, USA) for the generous gift of hrDecorin, and Peter Nightingale of University Hospital Birmingham for his statistical advice and the Biomedical Services Unit at the University of Birmingham for assistance with animal care.

Supported by grants from Biotechnology and Biological Sciences Research Council Doctoral Training (Grant number BB/F017553/1; Swindon, United Kingdom), and The School of Clinical and Experimental Medicine at the College of Medical and Dental Sciences, University of Birmingham (Edgbaston, Birmingham, UK).

Disclosure: **L.J. Hill**, None; **B. Mead**, None; **R.J. Blanch**, None; **Z. Ahmed**, None; **F. De Cogan**, None; **P.J. Morgan-Warren**, None; **S. Mohamed**, None; **W. Leadbeater**, None; **R.A.H. Scott**, None; **M. Berry**, None; **A. Logan**, None

References

1. Alvarado J, Murphy C, Juster R. Trabecular meshwork cellularity in primary open-angle glaucoma and nonglaucomatous normals. *Ophthalmology*. 1984;91:564–579.
2. Alvarado J, Murphy C, Polansky J, Juster R. Age-related changes in trabecular meshwork cellularity. *Invest Ophthalmol Vis Sci*. 1981;21:714–727.
3. Grierson I, Howes RC. Age-related depletion of the cell population in the human trabecular meshwork. *Eye*. 1987;1:204–210.
4. Tektas O-Y, Lütjen-Drecoll E. Structural changes of the trabecular meshwork in different kinds of glaucoma. *Exp Eye Res*. 2009;88:769–775.
5. Nakajima E, Nakajima T, Minagawa Y, Shearer TR, Azuma M. Contribution of ROCK in contraction of trabecular meshwork: proposed mechanism for regulating aqueous outflow in monkey and human eyes. *J Pharm Sci*. 2005;94:701–708.
6. Inoue T, Tanihara H. Rho-associated kinase inhibitors: a novel glaucoma therapy. *Prog Retin Eye Res*. 2013;37:1–12.
7. Borrás T. Gene expression in the trabecular meshwork and the influence of intraocular pressure. *Prog Retin Eye Res*. 2003;22:435–463.
8. WuDunn D. Mechanobiology of trabecular meshwork cells. *Exp Eye Res*. 2009;88:718–723.
9. Fleenor DL, Shepard AR, Hellberg PE, Jacobson N, Pang I-H, Clark AF. TGFβ2-induced changes in human trabecular meshwork: implications for intraocular pressure. *Invest Ophthalmol Vis Sci*. 2006;47:226–234.
10. Lütjen-Drecoll E, Shimizu T, Rohrbach M, Rohen J. Quantitative analysis of 'plaque material' in the inner-and outer wall of Schlemm's canal in normal-and glaucomatous eyes. *Exp Eye Res*. 1986;42:443–455.
11. Rohen J, Lütjen-Drecoll E, Flügel C, Meyer M, Grierson I. Ultrastructure of the trabecular meshwork in untreated cases of primary open-angle glaucoma (POAG). *Exp Eye Res*. 1993;56:683–692.
12. Ueda J, Wentz-Hunter K, Yue BY. Distribution of myocilin and extracellular matrix components in the juxtacanalicular tissue of human eyes. *Invest Ophthalmol Vis Sci*. 2002;43:1068–1076.
13. Lütjen-Drecoll E, Futa R, Rohen J. Ultrahistochemical studies on tangential sections of the trabecular meshwork in normal and glaucomatous eyes. *Invest Ophthalmol Vis Sci*. 1981;21:563–573.
14. Fuchshofer R, Welge-Lussen U, Lütjen-Drecoll E. The effect of TGF-β2 on human trabecular meshwork extracellular proteolytic system. *Exp Eye Res*. 2003;77:757–765.
15. Han H, Kampik D, Grehn F, Schlunck G. TGF-β2-induced invadosomes in human trabecular meshwork cells. *PLoS One*. 2013;8:e70595.
16. Junglas B, Kuespert S, Seleem AA, et al. Connective tissue growth factor causes glaucoma by modifying the actin cytoskeleton of the trabecular meshwork. *Am J Pathol*. 2012;180:2386–2403.
17. Kottler UB, Jünemann AGM, Aigner T, Zenkel M, Rummelt C, Schlötzer-Schrehardt U. Comparative effects of TGF-β1 and TGF-β2 on extracellular matrix production, proliferation, migration, and collagen contraction of human Tenon's capsule fibroblasts in pseudoexfoliation and primary open-angle glaucoma. *Exp Eye Res*. 2005;80:121–134.
18. Leivonen S-K, Lazaridis K, Decock J, Chantry A, Edwards DR, Kähäri V-M. TGF-β-elicited induction of tissue inhibitor of metalloproteinases (TIMP)-3 expression in fibroblasts involves complex interplay between Smad3, p38α, and ERK1/2. *PLoS One*. 2013;8:e57474.
19. Prendes MA, Harris A, Wirostko BM, Gerber AL, Siesky B. The role of transforming growth factor β in glaucoma and the therapeutic implications. *Br J Ophthalmol*. 2013;97:680–686.
20. Robertson JV, Golesic E, Gauldie J, West-Mays JA. Ocular gene transfer of active TGF-β induces changes in anterior segment morphology and elevated IOP in rats. *Invest Ophthalmol Vis Sci*. 2010;51:308–318.
21. Robertson JV, Siwakoti A, West-Mays JA. Altered expression of transforming growth factor beta 1 and matrix metalloproteinase-9 results in elevated intraocular pressure in mice. *Mol Vis*. 2013;19:684.
22. Shepard AR, Millar JC, Pang I-H, Jacobson N, Wang W-H, Clark AF. Adenoviral gene transfer of active human transforming growth factor-β2 elevates intraocular pressure and reduces outflow facility in rodent eyes. *Invest Ophthalmol Vis Sci*. 2010;51:2067–2076.
23. Taylor AW. Primary open-angle glaucoma: A transforming growth factor-β pathway–mediated disease. *Am J Pathol*. 2012;180:2201–2204.
24. Kottler UB, Jünemann AG, Aigner T, Zenkel M, Rummelt C, Schlötzer-Schrehardt U. Comparative effects of TGF-β1 and TGF-β2 on extracellular matrix production, proliferation, migration, and collagen contraction of human Tenon's capsule fibroblasts in pseudoexfoliation and primary open-angle glaucoma. *Exp Eye Res*. 2005;80:121–134.
25. Ochiai Y, Ochiai H. Higher concentration of transforming growth factor-β in aqueous humor of glaucomatous eyes and diabetic eyes. *Jpn J Ophthalmol*. 2002;46:249–253.
26. Picht G, Welge-Luessen U, Grehn F, Lütjen-Drecoll E. Transforming growth factor β2 levels in the aqueous humor in different types of glaucoma and the relation to filtering bleb development. *Graefes Arch Clin Exp*. 2001;239:199–207.
27. Tripathi RC, Chan WA, Li J, Tripathi BJ. Trabecular cells express the TGF-β2 gene and secrete the cytokine. *Exp Eye Res*. 1994;58:523–528.

28. Inatani M, Tanihara H, Katsuta H, Honjo M, Kido N, Honda Y. Transforming growth factor-β2 levels in aqueous humor of glaucomatous eyes. *Graefes Arch Clin Exp*. 2001;239:109–113.
29. Gottanka J, Chan D, Eichhorn M, Lütjen-Drecoll E, Ethier CR. Effects of TGF-β2 in perfused human eyes. *Invest Ophthalmol Vis Sci*. 2004;45:153–158.
30. Wordinger RJ, Fleenor DL, Hellberg PE, et al. Effects of TGF-β2, BMP-4, and gremlin in the trabecular meshwork: implications for glaucoma. *Invest Ophthalmol Vis Sci*. 2007;48:1191–1200.
31. Zhao X, Ramsey KE, Stephan DA, Russell P. Gene and protein expression changes in human trabecular meshwork cells treated with transforming growth factor-β. *Invest Ophthalmol Vis Sci*. 2004;45:4023–4034.
32. Sethi A, Mao W, Wordinger RJ, Clark AF. Transforming growth factor–β induces extracellular matrix protein cross-linking lysyl oxidase (LOX) genes in human trabecular meshwork cells. *Invest Ophthalmol Vis Sci*. 2011;52:5240–5250.
33. Baramova E, Bajou K, Remacle A, et al. Involvement of PA/plasmin system in the processing of pro-MMP-9 and in the second step of pro-MMP-2 activation. *FEBS Letters*. 1997;405:157–162.
34. Guo M-S, Wu Y-Y, Liang Z-B Hyaluronic acid increases MMP-2 and MMP-9 expressions in cultured trabecular meshwork cells from patients with primary open-angle glaucoma. *Mol Vis*. 2012;18:1175.
35. Borisuth N, Tripathi B, Tripathi R. Identification and partial characterization of TGF-β1 receptors on trabecular cells. *Invest Ophthalmol Vis Sci*. 1992;33:596–603.
36. Yang C, Houren W, Michael P, Banghong D, Zhongyu L. Apoptosis of human trabecular meshwork cells induced by transforming growth factor-β2 in vitro in vitro. *J Huazhong Univ Sci Technol Med Sci*. 2004;24:87–89.
37. Honjo M, Tanihara H, Inatani M, et al. Effects of rho-associated protein kinase inhibitor Y-27632 on intraocular pressure and outflow facility. *Invest Ophthalmol Vis Sci*. 2001;42:137–144.
38. Wiederholt M. Direct involvement of trabecular meshwork in the regulation of aqueous humor outflow. *Curr Opin Ophthalmol*. 1998;9:46–49.
39. Rao PV, Deng P, Sasaki Y, Epstein DL. Regulation of myosin light chain phosphorylation in the trabecular meshwork: role in aqueous humour outflow facility. *Exp Eye Res*. 2005;80:197–206.
40. Honjo M, Tanihara H, Inatani M, et al. Effects of rho-associated protein kinase inhibitor Y-27632 on intraocular pressure and outflow facility. *Invest Ophthalmol Vis Sci*. 2001;42:137–144.
41. Van de Velde S, Van Bergen T, Sijnave D, et al. AMA0076, a novel, locally acting Rho kinase inhibitor, potently lowers intraocular pressure in New Zealand white rabbits with minimal hyperemia. *Invest Ophthalmol Vis Sci*. 2014;55:1006–1016.
42. Yang C-YC, Liu Y, Lu Z, Ren R, Gong H. Effects of Y27632 on aqueous humor outflow facility with changes in hydrodynamic pattern and morphology in human eyes. *Invest Ophthalmol Vis Sci*. 2013;54:5859–5870.
43. Vidal-Sanz M, Salinas-Navarro M, Nadal-Nicolás FM, et al. Understanding glaucomatous damage: anatomical and functional data from ocular hypertensive rodent retinas. *Prog Retin Eye Res*. 2012;31:1–27.
44. Morrison JC, Johnson EC, Cepurna W, Jia L. Understanding mechanisms of pressure-induced optic nerve damage. *Prog Retin Eye Res*. 2005;24:217–240.
45. Almasieh M, Wilson AM, Morquette B, Vargas JLC, Di Polo A. The molecular basis of retinal ganglion cell death in glaucoma. *Prog Retin Eye Res*. 2012;31:152–181.
46. Dai C, Khaw PT, Yin ZQ, Li D, Raisman G, Li Y. Structural basis of glaucoma: the fortified astrocytes of the optic nerve head are the target of raised intraocular pressure. *Glia*. 2012;60:13–28.
47. Botfield H, Gonzalez AM, Abdullah O, et al. Decorin prevents the development of juvenile communicating hydrocephalus. *Brain*. 2013;136:2842–2858.
48. Logan A, Baird A, Berry M. Decorin attenuates gliotic scar formation in the rat cerebral hemisphere. *Exp Neurol*. 1999;159:504–510.
49. Schönherr E, O'Connell BC, Schittny J, et al. Paracrine or virus-mediated induction of decorin expression by endothelial cells contributes to tube formation and prevention of apoptosis in collagen lattices. *Eur J Cell Biol*. 1999;78:44–55.
50. Seidler DG, Goldoni S, Agnew C, et al. Decorin protein core inhibits in vivo cancer growth and metabolism by hindering epidermal growth factor receptor function and triggering apoptosis via caspase-3 activation. *J Biol Chem*. 2006;281:26408–26418.
51. Du S, Wang S, Wu Q, Hu J, Li T. Decorin inhibits angiogenic potential of choroid-retinal endothelial cells by downregulating hypoxia-induced Met, Rac1, HIF-1α and VEGF expression in cocultured retinal pigment epithelial cells. *Exp Eye Res*. 2013;116:151–160.
52. Schönherr E, Sunderkötter C, Iozzo RV, Schaefer L. Decorin, a novel player in the insulin-like growth factor system. *J Biol Chem*. 2005;280:15767–15772.
53. Svensson L, Heineg D. Decorin-binding sites for collagen type I are mainly located in leucine-rich repeats 4-5. *J Biol Chem*. 1995;270:20712–20716.
54. Ahmed Z, Bansal D, Tizzard K, et al. Decorin blocks scarring and cystic cavitation in acute and induces scar dissolution in chronic spinal cord wounds. *Neurobiol Dis*. 2014;64:163–176.
55. Davies JE, Tang X, Denning JW, Archibald SJ, Davies SJ. Decorin suppresses neurocan, brevican, phosphacan and NG2 expression and promotes axon growth across adult rat spinal cord injuries. *Eur J Neurosci*. 2004;19:1226–1242.
56. Nassar K, Lüke J, Lüke M, et al. The novel use of decorin in prevention of the development of proliferative vitreoretinopathy (PVR). *Graefes Arch Clin Exp*. 2011;249:1649–1660.
57. Isaka Y, Brees DK, Ikegaya K, et al. Gene therapy by skeletal muscle expression of decorin prevents fibrotic disease in rat kidney. *Nat Med*. 1996;2:418–423.
58. Giri SN, Hyde DM, Braun RK, Gaarde W, Harper JR, Pierschbacher MD. Antifibrotic effect of decorin in a bleomycin hamster model of lung fibrosis. *Biochem Pharmacol*. 1997;54:1205–1216.
59. Minor K, Tang X, Kahrilas G, Archibald SJ, Davies JE, Davies SJ. Decorin promotes robust axon growth on inhibitory CSPGs and myelin via a direct effect on neurons. *Neurobiol Dis*. 2008;32:88–95.
60. Tsuruga H, Murata H, Araie M, Aihara M. A model for the easy assessment of pressure-dependent damage to retinal ganglion cells using cyan fluorescent protein–expressing transgenic mice. *Mol Vis*. 2012;18:2468.
61. Surey S, Berry M, Logan A, Bicknell R, Ahmed Z. Differential cavitation, angiogenesis and wound-healing responses in injured mouse and rat spinal cords. *Neuroscience*. 2014;275:62–80.
62. Mead B, Thompson A, Scheven BA, Logan A, Berry M, Leadbeater W. Comparative evaluation of methods for estimating retinal ganglion cell loss in retinal sections and wholemounts. *PLoS One*. 2014;9:e110612.
63. Nakazawa T, Takahashi H, Nishijima K, et al. Pitavastatin prevents NMDA-induced retinal ganglion cell death by suppressing leukocyte recruitment. *J Neurochem*. 2007;100:1018–1031.
64. Vigneswara V, Akpan N, Berry M, Logan A, Troy CM, Ahmed Z. Combined suppression of CASP2 and CASP6 protects retinal

Investigative Ophthalmology & Visual Science

ganglion cells from apoptosis and promotes axon regeneration through CNTF-mediated JAK/STAT signalling. *Brain*. 2014; 137:1656–1675.

65. Belforte N, Sande P, de Zavalía N, Knepper PA, Rosenstein RE. Effect of chondroitin sulfate on intraocular pressure in rats. *Invest Ophthalmol Vis Sci*. 2010;51:5768–5775.
66. Nili N, Cheema AN, Giordano FJ, et al. Decorin inhibition of PDGF-stimulated vascular smooth muscle cell function: potential mechanism for inhibition of intimal hyperplasia after balloon angioplasty. *Am J Pathol*. 2003;163:869–878.
67. Ahmed Z, Bansal D, Tizzard K, et al. Decorin blocks scarring and cystic cavitation in acute and induces scar dissolution in chronic spinal cord wounds. *Neurobiol Dis*. 2014;64:163–176.
68. Grisanti S, Szurman P, Warga M, et al. Decorin modulates wound healing in experimental glaucoma filtration surgery: a pilot study. *Invest Ophthalmol Vis Sci*. 2005;46:191–196.
69. Rönkkö S, Rekonen P, Kaarniranta K, Puustjärvi T, Teräsvirta M, Uusitalo H. Matrix metalloproteinases and their inhibitors in the chamber angle of normal eyes and patients with primary open-angle glaucoma and exfoliation glaucoma. *Graefes Arch Clin Exp*. 2007;245:697–704.
70. Schlötzer-Schrehardt U, Lommatzsch J, Küchle M, Konstas AGP, Naumann GOH. Matrix metalloproteinases and their inhibitors in aqueous humor of patients with pseudoexfoliation syndrome/glaucoma and primary open-angle glaucoma. *Invest Ophthalmol Vis Sci*. 2003;44:1117–1125.
71. Yang J, Zhang K, Howard CP, et al. Serum matrix metalloproteinase levels and activities in patients with glaucoma. *Invest Ophthalmol Vis Sci*. 2003;44:102–B27.
72. Bradley JM, Kelley MJ, Rose A, Acott TS. Signalling pathways used in trabecular matrix metalloproteinase response to mechanical stretch. *Invest Ophthalmol Vis Sci*. 2003;44: 5174–5181.
73. De Groef L, Van Hove I, Dekeyster E, Stalmans I, Moons L. MMPs in the trabecular meshwork: promising targets for future glaucoma therapies? *Invest Ophthalmol Vis Sci*. 2013; 54:7756–7763.
74. Seidler DG, Schaefer L, Robenek H, Iozzo RV, Kresse H, Schönherr E. A physiologic three-dimensional cell culture system to investigate the role of decorin in matrix organisation and cell survival. *Biochem Biophys Res Commun*. 2005;332: 1162–1170.
75. Schönherr E, Levkau B, Schaefer L, Kresse H, Walsh K. Decorin-mediated signal transduction in endothelial cells involvement of Akt/protein kinase B in up-regulation of p21WAF1/CIP1 but not p27KIP1. *J Biol Chem*. 2001;276: 40687–40692.
76. Goldoni S, Iozzo RV. Tumor microenvironment: modulation by decorin and related molecules harboring leucine-rich tandem motifs. *Int J Cancer*. 2008;123:2473–2479.
77. Schaefer L, Macakova K, Raslik I, et al. Absence of decorin adversely influences tubulointerstitial fibrosis of the obstructed kidney by enhanced apoptosis and increased inflammatory reaction. *Am J Pathol*. 2002;160:1181–1191.
78. Wu H, Wang S, Xue A, et al. Overexpression of decorin induces apoptosis and cell growth arrest in cultured rat mesangial cells in vitro. *Nephrology*. 2008;13:607–615.
79. Tsai JC, Wu L, Worgul B, Forbes M, Cao J. Intravitreal administration of erythropoietin and preservation of retinal ganglion cells in an experimental rat model of glaucoma. *Curr Eye Res*. 2005;30:1025–1031.

Investigative Ophthalmology & Visual Science